THE JOURNAL OF BIOLOGICAL CHEMISTRY
Vol. 277, No. 14, Issue of April 5, pp. 11845–11852, 2002
Printed in U.S.A.


# Repair of Active and Silenced rDNA in Yeast

## THE CONTRIBUTIONS OF PHOTOLYASE AND TRANSCRIPTION-COUPLED NUCLEOTIDE EXCISION REPAIR*

Received for publication, November 15, 2001, and in revised form, January 4, 2002
Published, JBC Papers in Press, January 22, 2002, DOI 10.1074/jbc.M110941200

**Andreas Meier, Magdalena Livingstone-Zatchej, and Fritz Thoma‡**

*From the Institut für Zellbiologie, Departement Biologie, Eidgenössische Technische Hochschule (ETH), Hönggerberg, CH-8093 Zürich, Switzerland*

**DNA repair by photolyase (photoreactivation) and nucleotide excision repair (NER) are the major pathways to remove UV-induced cyclobutane-pyrimidine dimers (CPDs). The nucleolus is a nuclear subcompartment containing the ribosomal RNA genes (rDNA) of which a fraction is transcribed by RNA polymerase I (RNAP-I), and the rest is silenced. Here yeast was used to investigate how photoreactivation and NER contribute to repair of active and inactive rDNA. Cells were irradiated with UV light and exposed to different repair conditions. Nuclei were isolated, and the active genes were separated from the inactive genes by restriction endonuclease digestion. CPDs were measured in total rDNA, in both fractions, and in the *GAL10* gene. Repair in rDNA was as efficient as in *GAL10* indicating that both pathways have unrestricted access to the nucleolus. Photoreactivation was much faster than NER and therefore was the predominant repair pathway. Active genes were faster repaired by photolyase than were silenced genes providing evidence for an open chromatin structure during repair. The transcribed strands of active genes, but not of inactive genes, were slightly faster repaired by NER providing evidence for transcription-coupled repair by RNAP-I. There was no pronounced inhibition of photoreactivation by RNAP-I in the transcribed strand, which is in contrast to genes transcribed by RNAP-II and suggests different stabilities of RNAP-I and RNAP-II stalled at CPDs.**

Repair of DNA lesions is essential to prevent mutations, cell death, or cancer (1). Since packaging of eukaryotic DNA in nucleosomes and higher order chromatin structures restricts DNA accessibility, all DNA-dependent processes including repair and transcription are mutually affected by structural and dynamic properties of chromatin (2–4). Here we investigated how two different repair mechanisms, photoreactivation and nucleotide excision repair (NER),[1] find access to ribosomal DNA and repair UV lesions in the nucleolus of yeast cells.

NER and photoreactivation are the major pathways to remove UV-induced DNA lesions, *cis-syn* cyclobutane-pyrimidine dimers (CPDs), and pyrimidine-pyrimidone (6-4) photoproducts (6-4PPs) (5). Photoreactivation is a direct repair mechanism where a damage-specific enzyme (photolyase) reverts CPDs in a light-dependent reaction. Photolyases are found in many prokaryotes and eukaryotes, including yeast (5–8). Photoreactivation in yeast cells is modulated by chromatin structure and transcription (2). Photolyase is fast in nucleosome-free regions and slow in nucleosomes and therefore is an ideal molecular tool to investigate DNA accessibility in chromatin of living cells (9–11). There is preferential repair of the nontranscribed strands in genes transcribed by RNAP-II and RNAP-III, whereas photoreactivation of the transcribed strands is partially inhibited by RNAP-II and RNAP-III blocked at CPDs (9, 12, 13).

In contrast to photolyase, NER is a multistep mechanism that removes a large range of DNA lesions including CPDs and 6-4PPs (5). NER is divided in two subpathways, global genome repair and transcription-coupled repair (1, 14–16). Global genome repair refers to repair in nontranscribed parts of the genome and is modulated by nucleosomes (17, 18) and other protein/DNA interactions (11, 12, 19, 20). Transcription-coupled repair refers to preferential repair of the transcribed strand, an observation that was originally made in mammalian and hamster cells (21) and later in many more organisms including yeast (22, 23). RNAP-II stalled at a DNA lesion may serve as a damage recognition enzyme and promote NER (1, 16). Transcription-coupled repair was found in genes transcribed by RNAP-II, while genes transcribed by RNAP-III lack transcription-coupled repair in mammalian cells (24) and show a slight inhibition of NER on the transcribed strand in yeast (12).

The nucleolus is a subcompartment of the nucleus specialized in biosynthesis of ribosomes, a dense, protein crowded factory of transcription, RNA-processing and ribosome assembly (25). It harbors the clusters of rRNA genes (rDNA) coding for the large ribosomal RNA transcripts. rDNA is transcribed by RNAP-I, but only a fraction of the genes is active. Active genes are free of nucleosomes, while silenced genes maintain nucleosomes (26–28). Repair of UV lesions in ribosomal genes is still not clear. Removal of CPDs by NER was absent in rodent cells and inefficient in human cells (29–31). 6-4PPs, however, were efficiently repaired (32). NER of mammalian rDNA showed no strand bias and appears therefore not to be coupled to RNAP-I transcription (29, 30). Repair of rDNA in yeast *Saccharomyces cerevisiae* is different. First, CPDs are efficiently removed by NER. Second, experiments with mutants that compromise global genome repair revealed preferential repair of the transcribed strand and suggested that TC NER may exist in rDNA transcribed by RNAP-I (33). Since that study analyzed the total rDNA population and did not discriminate between actively transcribed and silenced genes, it re-

* This work was supported by grants from the Swiss National Science Foundation and the ETH Zürich, the Roche Research Foundation, and the Janggen-Pöhn-Stifung. The costs of publication of this article were defrayed in part by the payment of page charges. This article must therefore be hereby marked "*advertisement*" in accordance with 18 U.S.C. Section 1734 solely to indicate this fact.

‡ To whom correspondence should be addressed: Institut für Zellbiologie, ETH-Hönggerberg, CH-8093 Zürich, Switzerland. Tel.: 41-1-6333323; Fax: 41-1-6331069; E-mail: thoma@cell.biol.ethz.ch.

[1] The abbreviations used are: NER, nucleotide excision repair; CPD, cyclobutane-pyrimidine dimer; rDNA, ribosomal DNA; RNAP, RNA polymerase; 6-4PP, pyrimidine-pyrimidone (6-4) photoproduct; MOPS, 4-morpholinepropanesulfonic acid; IRF, intact restriction fragment; s, slow (active); f, fast (inactive).

mains open whether the strand bias is related to transcription. In contrast to NER, photoreactivation or the combination of photoreactivation and NER were never investigated in the nucleolus.

Here we have investigated repair of UV lesions by both pathways in total rDNA as well as in the separated active and inactive rRNA genes. We found that photoreactivation is the predominant pathway for CPD repair in all situations. Moreover, we noticed that preferential repair of the transcribed strand by NER is restricted to the active rRNA genes thus supporting transcription-coupled repair. In addition, we observed structural changes in chromatin following damage induction and repair, but the active genes remained in a relatively open conformation.

## MATERIALS AND METHODS

*Yeast Strains*—*S. cerevisiae* W303.1a (*Mat**a***, *ade2-1*, *ura3-1*, *his3-11*,*15*, *trp1-1*, *leu2-3*,*112*, *can1-100*) was kindly provided by Dr. R. Sternglanz. AMY3 (*Mat**a***, *ade2-1*, *ura3-1*, *his3-11*,*15*, *trp1-1*, *leu2-3*,*112*, *can1-100 rad1*::*URA3*) was generated by deletion of part of the *RAD1* gene in W303.1a using construct pR1.6 (kindly provided by Dr. L. Prakash). AMY3 exhibits a strong UV sensitivity typical for *rad1* strains.

*UV Irradiation and Repair*—UV irradiation and repair of DNA was done as described previously (34). Yeast cultures were grown at 30 °C in YPD (1% Bacto yeast extract, 1% Bacto peptone, 2% dextrose) (35) to a density of about $0.5 \times 10^7$ cells/ml. Cells were harvested and resuspended in SD minimal medium (2% dextrose, 0.67% yeast nitrogen base without amino acids) to about $3 \times 10^7$ cells/ml. 4-mm-deep suspensions were irradiated with UV light using Sylvania G15T8 germicidal lamps (predominantly at 254 nm) at a dose of 150 J/m$^2$ (measured by a UVX radiometer, UVP Inc., San Gabriel, CA). After irradiation, the medium was supplemented with appropriate amino acids and uracil. For photoreactivation, the cell suspension was exposed to photoreactivating light (Sylvania type F15 T8/BLB bulbs, peak emission at 375 nm) at ~1.3 milliwatts/cm$^2$ (measured by a UVX radiometer (UVP Inc.) with a 365 nm photocell) for 7–120 min at 24–26 °C. During incubation, the cells were repeatedly resuspended. NER samples were incubated at 24–26 °C in the dark. 100-ml samples were collected at different repair times and chilled on ice. All further steps until lysis of cells were performed in yellow safety light.

*Fractionation of Active and Inactive rDNA*—Yeast nuclei were liberated by glass bead isolation according to Muller *et al.* (36). Briefly, 100 ml of cells ($3 \times 10^7$ cells/ml) were harvested, resuspended in cold water, and resuspended in 2 ml of cold NIB (nuclear isolation buffer: 17% glycerol, 50 mM MOPS, 150 mM potassium acetate, 2 mM $MgCl_2$, 0.5 mM spermidine, 0.15 mM spermine, all adjusted to pH 7.2). The suspension was vortexed with 2 ml of glass beads (diameter, 0.5 mm; acid washed and equilibrated in NIB) until about 90% of the cells were broken (checked under light microscope for loss of contrast of broken cells). The nuclear extract was pelleted (10 min, 4 °C, $4500 \times g$) and resuspended in 2 ml of restriction buffer (33 mM Tris acetate, 10 mM magnesium acetate, 66 mM potassium acetate, 100 $\mu$g/ml bovine serum albumin, pH 7.9). Aliquots of $1.5 \times 10^9$ cells were digested with 160 units of *Nhe*I (AGS, Heidelberg, Germany) at 37 °C for 1 h to release the active ribosomal genes. No NER activity was observed during incubation of the extract at 37 °C (data not shown). Genomic DNA was extracted following the Yeast DNA Isolation Protocol (Qiagen Genomic DNA Handbook, 1999) and electrophoresed at 4 °C on 0.8% low melting agarose gels (SeaPlaque agarose, FMC BioProducts), and the fragments corresponding to active (4.4 kb) and inactive rDNA (>9.1kb) were purified according to the AgarACE protocol (Promega). The fractions were redigested with *Nhe*I (Roche Molecular Biochemicals) and purified by phenol extraction, and CPDs were analyzed.

*Psoralen Cross-linking and Gel Retardation Assays*—These assays were adopted from Muller *et al.* (36). *Nhe*I-digested yeast nuclei of $2–4 \times 10^8$ cells were centrifuged (8 min at $3400 \times g$, 4 °C) and resuspended in 300 $\mu$l of NIB. The suspension was transferred to wells of a multiwell dish (diameter, 1.6 cm) and placed on ice. 15 $\mu$l of 4,5′,8-trimethylpsoralen (Sigma, 200 $\mu$g/ml in ethanol) were added. After 5 min of incubation in the dark, the cells were irradiated on ice for 15 min (Sylvania, Type F15 T8/BLB bulbs, peak emission at 375 nm) at an average flux of about 24 J/m$^2$ s. This procedure was repeated four times. The cross-linked nuclear extract was pelleted and resuspended in 400 $\mu$l of TNE (50 mM Tris-HCl, pH 7.5, 10 mM EDTA, 100 mM NaCl). 40 $\mu$l of 16.5% sarcosyl (Sigma) and 30 $\mu$l of Proteinase K (10 mg/ml) were added and incubated for 2.5 h at 50 °C. After centrifugation for 5 min at 5000 rpm, the DNA was purified by phenol extraction and resuspended in 300 $\mu$l of TNE. After digestion with 10 $\mu$l of RNase A (10 mg/ml) for 20 min at 37 °C, the DNA was phenol-extracted and resuspended in 50 $\mu$l of 10 mM Tris, 0.5 mM EDTA, pH 7.5. The DNA was digested with *Bam*HI or *Nhe*I and separated on 1% agarose gels in 40 mM Tris, pH 7.6, 0.114% acetic acid, 1 mM EDTA for 20 h at 64 V. The psoralen cross-links were reversed by irradiation with 254 nm light (about 30 J/m$^2$ s) for 12 min, and the DNA was depurinated in 0.25 N HCl for 12 min, blotted to Zeta GT nylon membranes, and hybridized with radioactive probes according a protocol from Bio-Rad.

*CPD Analysis*—CPDs were analyzed by indirect end labeling (22) in the 4.4-kb rDNA fragment (DNA cut with *Nhe*I) and in the 1.6-kb *GAL10* fragment (DNA cut with *Eco*RI/*Sal*I). Aliquots of DNA were incubated for 2 h at 37 °C with T4 endonuclease V (Epicentre) in 50 mM Tris, 5 mM EDTA, pH 7.5, or mock-treated with the same buffer. The DNA was electrophoresed on 1.5% alkaline agarose gels, blotted to Zeta GT nylon membranes, and hybridized with radioactively labeled strand-specific DNA probes that abut the restriction site (34).

*Radioactive Probes*—DNA fragments for generation of radioactive probes were generated by whole cell PCR. The oligonucleotides used for the 387-bp rDNA probe contained 5′-AGTTCCTCTAAATGACCAAGT-3′ (top strand) and 5′-AGTTCCTCTAAATGACCAAGT-3′ (bottom strand). The oligonucleotides used for the 225-bp *GAL10* probe contained 5′-CGCACCATAATCTCCGTACCCTCAATAG-3′ (top strand) and 5′-CCGCCGAGTACATGCTGATAGATAATGA-3′ (bottom strand). Strand-specific probes were generated by primer extension with one oligonucleotide for each strand using Qiagen *Taq* polymerase. Probes for both strands were generated by random priming using the oligolabeling kit (Amersham Biosciences).

*Quantifications*—The signal on the membranes was quantified using a PhosphorImager (Molecular Dynamics). In each lane, the signal in the intact restriction fragment (IRF) was measured and divided by the signal of the whole lane to give a signal normalized with respect to the overall DNA content in that lane. CPD content was calculated using the Poisson expression (21): $-\ln(\text{IRF}(+\text{T4})/\text{IRF}(-\text{T4}))$. Initial damage (0 min repair) was set to 0% repair.

## RESULTS

We used the yeast strains AMY3 (*rad1*Δ) with an inactivated NER to analyze photoreactivation and W303.1a for analysis of NER and NER with photoreactivation. Cells were grown in YPD, irradiated with 150 J/m$^2$ in minimal medium containing glucose, and exposed to photoreactivating light for up to 2 h in minimal medium supplemented with the appropriate amino acids. For NER, the cultures were incubated in the dark. Since photoreactivation is a very fast process, photoreactivation and NER were done at 24–26 °C and not at 30 °C. To investigate repair of the total rDNA cluster, DNA was isolated and cut with *Nhe*I, which generates a 4.4-kb fragment of the transcribed region and a 4.7-kb fragment containing the 5′-end of the rRNA gene and the spacer (Fig. 1*A*). To detect the CPDs, the DNA was cut with T4 endonuclease V at CPDs, fractionated by alkaline agarose gel electrophoresis, blotted to a nylon membrane, and hybridized to strand-specific probes abutting from the *Nhe*I site (*black bar*, Fig. 1*A*). This indirect end-labeling technique allows the mapping of CPDs along the DNA sequence and the measurement of the fraction of undamaged restriction fragments (9, 17, 22, 34).

A set of data is shown for AMY3 (*rad1*Δ) and W303.1a (*RAD1*) (Fig. 1, *B* and *C*). Nonirradiated DNA (−UV) and DNA not treated with T4 endonuclease V (−T4) show the intact restriction fragment (4.4 kb, *top band*). Treatment of damaged DNA with T4 endonuclease V generated a smear with some bands, which represent the distribution of pyrimidine clusters (+UV, +T4). The CPD patterns are different in the nontranscribed strand and the transcribed strand demonstrating strand specificity of the assay. The *top band* (4.4 kb) represents the fraction of undamaged DNA. The initial damage was on average 0.17 ± 0.03 CPDs/kb in the nontranscribed strand and 0.2 ± 0.04 CPDs/kb in the transcribed strand probably reflect-

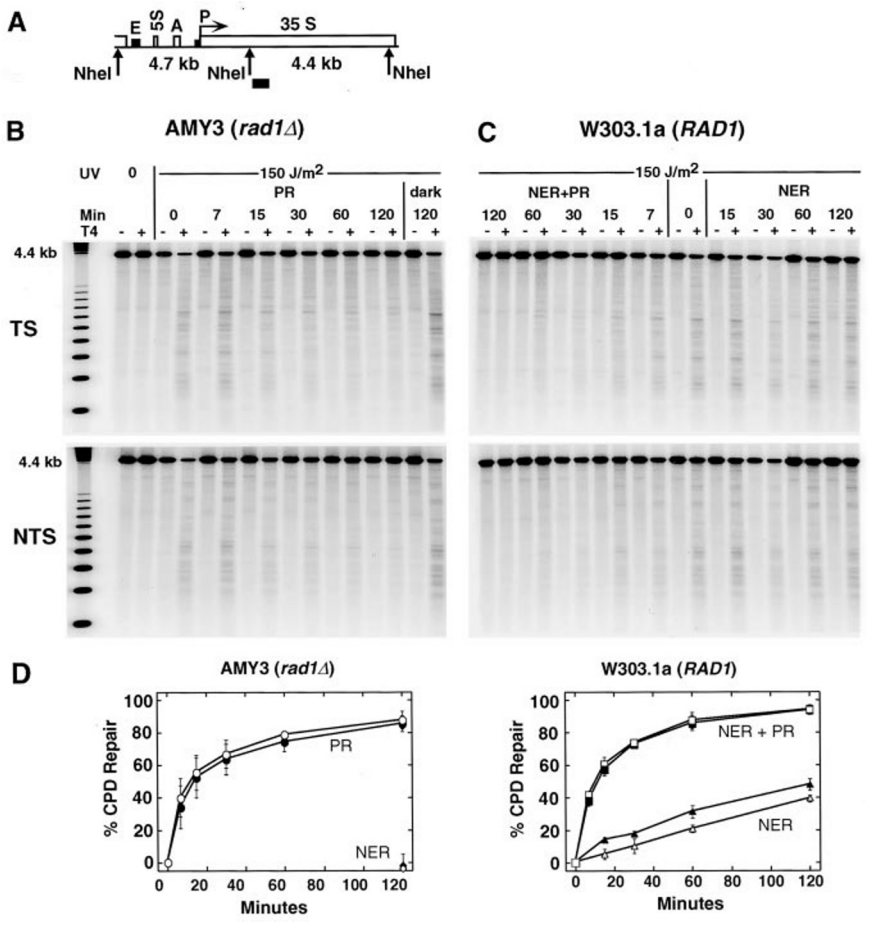


FIG. 1. **CPD repair in yeast rDNA.** *A*, schematic view of rDNA repeat containing the 35 S ribosomal RNA gene (*35S*) with the promoter (*P*) and the spacer with the enhancer (*E*), the 5 S rRNA gene (*5S*), and the ribosomal origin of replication (*A*). *4.7 kb* and *4.4 kb* are restriction fragments generated by *Nhe*I. *Black bar*, rDNA probe used for hybridization. *B*, photoreactivation (*PR*) in AMY3 (*rad1*Δ). *C*, NER and NER + photoreactivation (*PR*) in W303.1a (*RAD1*). Cells were grown in glucose, irradiated with ultraviolet light (150 J/m$^2$, *UV*), exposed to photoreactivating light for 7, 15, 30, 60, and 120 min (*PR*, *Min*) or kept in the dark for 15–120 min to allow NER. DNA was extracted and cut with *Nhe*I. DNA was cut at CPDs with T4 endonuclease V (+*T4*) or mock-treated (−*T4*), fractionated by alkaline agarose gel electrophoresis, blotted, and hybridized with strand-specific probes (*black bar* in *A*) to detect the 4.4-kb fragment. *TS*, transcribed strand; *NTS*, nontranscribed strand. *D*, repair curves. The curves are averages of three independent UV experiments and at least two gels per UV experiment. *Open symbols*, nontranscribed strand; *filled symbols*, transcribed strand; *circles*, photoreactivation; *diamonds*, NER in AMY3; *squares*, NER and photoreactivation; *triangles*, NER in W303.1a.

ing a difference in the pyrimidine distribution. The relative low levels of CPDs/kb generated by 150 J/m$^2$ was due to the irradiation of cells in SD medium. According to the Poisson distribution, ~75% of the genes contained one or more transcription-blocking CPDs in the transcribed strand (6.6 kb).

*Photoreactivation Is the Predominant Pathway to Remove CPDs from the Nucleolus*—Repair of CPDs is visualized by a time-dependent decrease of the CPD bands and an increase of the intact 4.4-kb restriction fragment (Fig. 1, *B* and *C*). The removal of CPDs was homogenous. There are no sites that were resistant to repair. DNA repair of the whole 4.4-kb fragment was quantified, and the average of three independent experiments is displayed in Fig. 1*D*. AMY3 (*rad1*Δ) revealed very efficient repair by photolyase on both strands. About 50% of the lesions were removed by exposing cells to photoreactivating light for 15 min, and more than 80% of the lesions were removed in 2 h. No repair was observed when cells were kept in the dark demonstrating that the NER pathway was inactivated. Repair in the NER-proficient strain W303.1a showed slow removal of CPDs by NER when cells were incubated in the dark. A substantial fraction of lesions (about 60%) remained unrepaired after 2 h. Please note that NER was slow since the experiments were done at low temperature (24–26 °C). In contrast, exposure of those cells to photoreactivating light showed that the combination of NER and photoreactivation very rapidly removed CPDs. 50% of the lesions were repaired in less than 15 min. This experiment demonstrates that both pathways repair CPDs in the nucleolus, but photoreactivation is the predominant pathway under the light conditions applied in those experiments.

*A Strand Bias of NER Indicates Transcription-coupled Repair in rDNA*—It was previously reported that the transcribed strand of total rDNA was slightly faster repaired than the nontranscribed strand suggesting transcription-coupled NER (33). Consistent with that report, we observed preferential repair of the transcribed strand by NER as well (Fig. 1*D*). The difference between the two strands is small compared with the strand bias observed in genes transcribed by RNAP-II (13). This might reflect either a small number of active genes in the rDNA population, or transcription-coupled repair might be less pronounced compared with RNAP-II-transcribed genes. To address this topic, we investigated repair in active and inactive fractions separately.

*Isolation of DNA from Active and Inactive rDNA*—Psoralen cross-linking and nuclease digestion studies have established that actively transcribed rDNA is devoid of nucleosomes, while inactive genes are packaged in nucleosomes (27, 28, 37). It was further shown that restriction enzymes such as *Nhe*I efficiently cut in active rRNA genes of yeast but not in the inactive nucleosomal genes (36). We used this approach to purify DNA fragments of active genes for repair analysis. Yeast cells were UV-irradiated and incubated for repair as described above. Nuclei were isolated and digested with *Nhe*I, which liberates a 4.4-kb fragment of active rDNA (Fig. 2*A*). The DNA of *Nhe*I-digested nuclei was purified and fractionated in neutral agarose gels, and the rDNA fragments were identified after blotting using an rDNA probe, which hybridized to the 4.4-kb *Nhe*I fragment (Fig. 2*B*). The DNA originating from inactive genes, which were resistant to *Nhe*I digestion, showed up as long DNA fragments (>9.1 kb, inactive fraction of rDNA). The 9.1-kb fragment was a partial digest of two adjacent active genes and was not further used for repair analysis. The fraction of active genes that was released by *Nhe*I is represented by the 4.4-kb band.

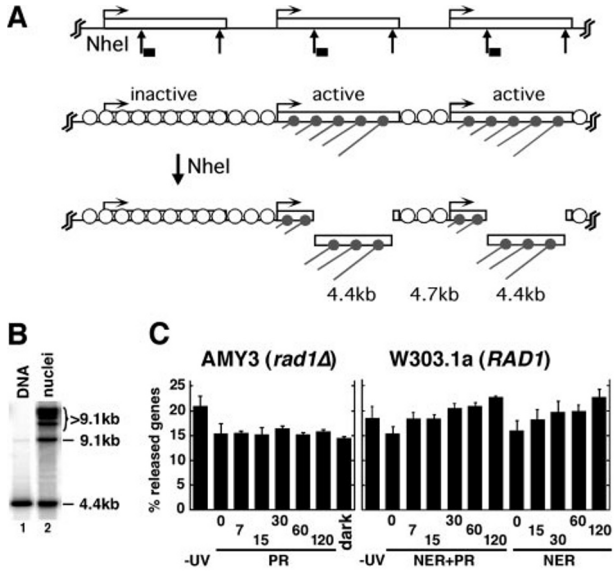


FIG. 2. **Separation of active and inactive rRNA genes after damage induction and repair.** *A*, three units of rDNA are shown schematically. Active genes are transcribed by RNAP-I and free of nucleosomes; inactive genes and the spacer are packaged in nucleosomes (*circles*). Active genes are efficiently cut by *Nhe*I in nuclei to release a 4.4-kb chromatin fragment. Inactive genes are resistant to *Nhe*I digestion (36). *B*, nuclei were digested with *Nhe*I, the DNA was purified, and the fragments were identified by Southern blotting using the rDNA probe (*black bar* in *A*). 4.4-kb band represents the released rDNA of active genes, the 9.1-kb band originates from a partial digest of two active genes, and fragments longer than 9.1 kb contain the inactive genes. *Lane 1*, genomic DNA cut with *Nhe*I; *lane 2*, DNA of *Nhe*I-digested nuclei of AMY3. *C*, the fraction of 4.4-kb fragments released by *Nhe*I is shown as the average of three independent experiments with AMY3 and W303.1a. *PR*, photoreactivation.

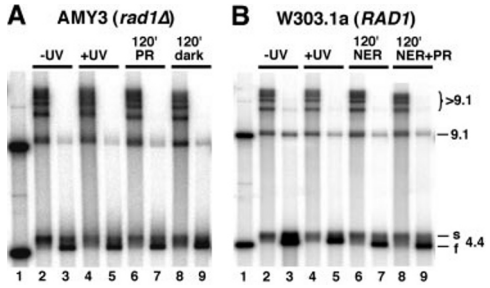


FIG. 3. **Psoralen cross-linking of *Nhe*I-digested nuclei.** Only active rDNA is released by *Nhe*I digestion. *A*, AMY3 (*rad1*Δ). *B*, W303.1a (*RAD1*). Nuclei were digested with *Nhe*I and cross-linked with trimethylpsoralen. The DNA was analyzed by Southern blotting using the rDNA probe (Fig. 2*A*) (*lanes 2*, *4*, *6*, and *8*). An aliquot of DNA was cut to completion with *Nhe*I (*lanes 3*, *5*, *7*, and *9*) prior to analysis. Samples are shown for unirradiated cells (−*UV*), after damage induction (+*UV*), and after 120-min exposure to repair conditions (*PR*, *dark*, *NER*, and *NER* + *PR*). Non-nucleosomal DNA of active genes migrates slowly (s-band, *s*), and nucleosomal DNA of silenced genes migrates fast (f-band, *f*) (27, 37). Please note that more DNA was loaded in *lane 3* (*B*). *PR*, photoreactivation.

*Altered Chromatin Accessibility Induced by UV Irradiation and Repair*—If UV lesions block transcription elongation of RNAP-I, one might expect that inactivation could lead to a reformation of nucleosomes in rDNA and make it less accessible to restriction enzymes. We therefore measured the fraction of 4.4-kb fragments released by *Nhe*I during the repair experiments. In unirradiated cells, this fraction was about 20% of total rDNA (Fig. 2*C*, −*UV*). After UV irradiation, the fraction decreased indicating that UV-irradiated chromatin became less accessible to the restriction endonuclease (0 min repair). The decrease was only about 25%, although ~75% of the genes received at least one transcription-blocking CPD in the transcribed strand. Thus, damage induction in transcribed genes altered the structure of some genes but was not sufficient to generate a chromatin structure that was as resistant to nuclease digestion as inactive nucleosomal rDNA. Hence, a large fraction of the active genes remained in a partially open chromatin conformation.

In W303.1a, which is proficient in NER and photoreactivation, the fraction of released genes increased with increasing repair times in the presence and absence of photoreactivating light (Fig. 2*C*). However, in the NER-deficient AMY3 cells no increase of the released fraction was observed during exposure to photoreactivating light. The effects were small, but they were observed in all three independent experiments. Thus, the increased release in W303.1a cells suggests that some rRNA genes may open chromatin either as a consequence of repair within the gene or as a consequence of repair in other genes (see "Discussion"). Since yeast photolyase in contrast to NER does not repair 6-4PPs, the increased accessibility to *Nhe*I might depend on removal of that photoproduct.

*NheI Digestion of Nuclei Releases Only Open and Active rDNA*—Active genes with an open chromatin structure bind more psoralen than nucleosomal inactive genes leading to different gel retardation of the cross-linked active DNA (slow migration, s-band) and inactive DNA (fast migration, f-band) (26, 27). We used this approach to characterize chromatin structure of the released fragments in *Nhe*I-digested nuclei (Fig. 3). *Lanes 3* in AMY3 and W303.1a show cross-linked DNA that was isolated from *Nhe*I-treated nuclei and redigested to completion with *Nhe*I. Two bands (*s* and *f*) are observed at 4.4 kb that shifted with respect to uncross-linked DNA (*lanes 1*). The intensities of both bands illustrate that about 40% of total rDNA was in an open and active conformation (s-band), while the major fraction was inactive and packaged in nucleosomes (f-band).

*Lanes 2* in Fig. 3 show DNA fragments that were cross-linked after *Nhe*I digestion of nuclei. Only the s-band is visible at 4.4 kb demonstrating that only DNA of active genes was released by *Nhe*I digestion. The released active rDNA represents about 65% of total active rDNA. Since ~25% of active rDNA is found in the partial digests (9.1 kb), we estimate that the inactive rDNA (>9.1 kb) contains less than 10% of the active genes. *Lanes 5*, *7*, and *9* show the total fraction of active (*s*) and inactive (*f*) rDNA after damage formation and repair. Active rDNA remains a minor fraction throughout the experiment. *Lanes 4*, *6*, and *8* show the products of *Nhe*I-digested nuclei. No f-bands are detected demonstrating that only active and no inactive rDNA was released by *Nhe*I digestion.

We also noticed some subtle differences in psoralen cross-linking that might suggest that chromatin structure changes after damage induction and during repair (Fig. 3). First, while DNA released by *Nhe*I from nonirradiated cells showed a heavily cross-linked band typical for active genes (*lanes 2*), the DNA released from irradiated and repaired cells revealed a broader band reflecting a more heterogeneous population of cross-linked material (*lanes 4*). This indicates that a fraction of the genes is less accessible to psoralen and might have been partially refolded in nucleosomes. However, it is important to realize that UV irradiation did not result in a complete reformation of nucleosomes on transcribed genes. Thus, the released genes remained in a relatively open conformation. Second, psoralen cross-linking at different repair times indicates that the slow band characteristic for active genes is regenerated to some extent during repair. This is observed for NER and NER with photoreactivation (Fig. 3*B*, *lanes 6* and *8*) and for photoreactivation alone (Fig. 3*A*, *lane 6*) but not in the absence of repair (Fig. 3*A*, *lane 8*). Thus, the psoralen cross-linking data suggest

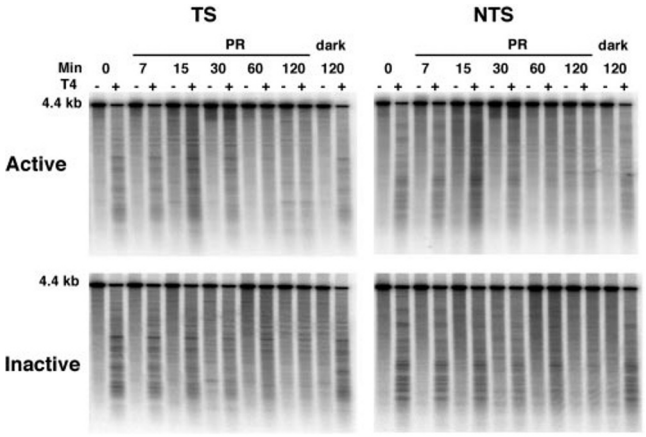


FIG. 4. **Photoreactivation in transcriptionally active and inactive fractions of rDNA of AMY3 (*rad1*Δ).** Repair conditions and digestion of nuclei were as described in Figs. 1 and 2. The 4.4-kb band of released active genes and the inactive rDNA (>9.1 kb) were purified from preparative gels, and the CPDs were analyzed as described in Fig. 1. *Active*, active rDNA; *Inactive*, inactive rDNA; *TS*, transcribed strand; *NTS*, nontranscribed strand; *PR*, photoreactivation; *+T4* and *−T4*, DNA treated with T4 endonuclease V or mock-treated, respectively.

that structural transitions occur in chromatin as a consequence of UV irradiation and repair. The structural basis and the mechanism of those transitions will be investigated in more detailed experiments.

*Photoreactivation Is the Predominant Pathway of CPD Repair in the Active and Inactive Genes*—For analysis of DNA damage and repair, the 4.4-kb *Nhe*I fragment of the active rDNA and the longer fragments of the inactive rDNA (>9.1 kb) were purified from preparative agarose gels (as shown in Fig. 2), redigested to completion with *Nhe*I, and analyzed as described in Fig. 1. The active fraction contains only active (open) genes (see above), while the inactive fraction may still contain DNA of a few active genes. Figs. 4 and 5 show representative sets of data for AMY3 and W303.1a, respectively, and the quantifications are presented in Fig. 6. It is obvious from the gels and repair curves that NER was slow. Only about 40% of CPDs were removed in 2 h, while photoreactivation or photoreactivation together with NER repaired about 80–90% of CPDs. Thus, photoreactivation is the predominant CPD repair pathway in active and inactive genes of the nucleolus.

*Enhanced Repair of Active Genes Implies That Chromatin Structure Remains Open during Repair*—Previous experiments have established that photoreactivation of the nontranscribed strand is sensitive to nucleosomes, while repair of the transcribed strand is inhibited by stalled RNA polymerases (9, 12, 13). Analysis of the nontranscribed strand of rDNA reveals that the active fraction was faster repaired by photolyase than were the silenced genes or total rDNA. In 15 min, photolyase alone removed about 68 ± 14% of CPDs from the active genes and 45 ± 7% from the silenced genes (Fig. 6). NER and photoreactivation together also removed about 66 ± 9 and 52 ± 3% from active and inactive genes, respectively, demonstrating that the contribution of NER to CPD repair is minimal in the first few minutes. The difference in repair of both fractions by NER alone is less pronounced. In 2 h, NER removes 46 ± 6% of the CPDs in the active fraction (nontranscribed strand) and 40 ± 8% in the silenced fraction. Thus, the repair results provide direct *in vivo* evidence that the active genes are in an open conformation and remain preferentially accessible after damage induction and during repair. In contrast, repair of the inactive genes is partially inhibited presumably due to their packaging into nucleosomes.

*A Strand Bias in Repair of Active Genes Is Consistent with Transcription-coupled NER and an Inhibition of Photolyase by RNAP-I*—NER shows preferential repair of the transcribed strand in the active fraction. No strand bias was observed in the inactive fraction (Fig. 6, *B* and *D*). This is an indication that RNAP-I promotes repair of CPDs by NER in the transcribed strand, a phenomenon called transcription-coupled repair. On the other hand, photoreactivation is slightly slower in the transcribed strand, and again this strand bias was not measured in the inactive fractions (Fig. 6, *A* and *C*). Therefore, RNAP-I blocked at CPDs might inhibit CPD repair by photolyase as it was observed in genes transcribed by RNAP-II and RNAP-III (12, 13). The strand bias of photoreactivation and NER in rDNA was small, but it was reproducibly observed in all three independent experiments. The error bars (Fig. 6) obtained by averaging the individual data points of all independent experiments overlap since the absolute repair values were slightly different in the different UV experiments, but the relative values (*e.g.* nontranscribed strand *versus* transcribed strand) were not changed. Summarizing the results of fractionated rDNA (Figs. 4, 5, and 6) and total rDNA (Fig. 1), we conclude that there is a contribution of transcription-coupled repair and an inhibition of photolyase by RNAP-I to DNA repair of rDNA.

*Unrestricted Access of Repair Enzymes to the Nucleolus*—Having observed efficient repair in the nucleolus, we investigated how nucleolar repair compares with repair of a genomic locus outside of the nucleolus. Fig. 7 shows a comparison of photoreactivation (AMY3) and NER (W303.1) between the rDNA and the *GAL10* gene. The *GAL10* gene was chosen since it is repressed and folded in nucleosomes when cells are grown in glucose (38). Repair of *GAL10* was analyzed by indirect end labeling as described previously (not shown) (13). The data reveal that photoreactivation of rDNA is slightly faster than photoreactivation of *GAL10*, and there is no dramatic difference in NER. Thus, the yeast nucleolus does not play an inhibitory role with respect to the accessibility of repair proteins.

## DISCUSSION

Yeast *S. cerevisiae* has two mechanisms to repair UV-induced DNA lesions, photoreactivation and NER (8). Photoreactivation was shown to be more efficient than NER and appeared to be the predominant pathway for CPD repair, while NER is required to remove non-CPD lesions (2, 9, 12, 13). Here we show that photoreactivation is also the predominant pathway for CPD repair in the nucleolus in the active and silenced rRNA genes. The predominance of photoreactivation depends on the light conditions, which probably are saturating in our experiments. At dim light conditions, however, NER might become the predominant pathway.

In yeast, the nucleolus is a morphologically distinct compartment that covers about a third of the nucleus, contains fibrillar centers, a dense fibrillar component, and granular components similar to that of higher eukaryotes, and appears morphologically more compact than the rest of the nucleus (25, 39). We have shown that NER repairs rDNA as efficiently as the inactive *GAL10* gene, which is located on chromosome II outside of the nucleolus, and photoreactivation is even faster (Fig. 7). Thus, despite the compartmentalization, the components of both pathways find unrestricted access to nucleolar chromatin. It is interesting to note that CPDs are inefficiently removed by NER in human and hamster cells, but strand breaks in human cells and 6-4PPs, intrastrand adducts, and interstrand crosslinks in rodent cells are more efficiently repaired (29, 30, 32, 40–42). Thus, DNA repair in nucleoli appears not to be directly related to nucleolar compartmentalization but rather to the specific properties of damage recognition and processing by the different repair pathways.

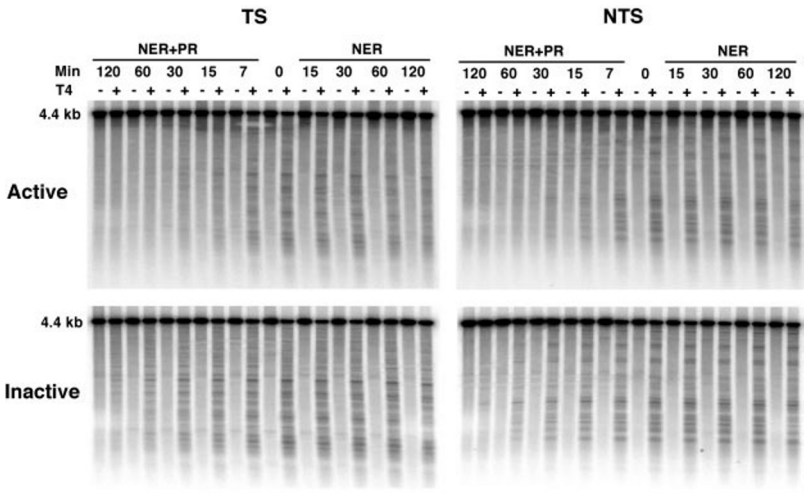


FIG. 5. **NER and NER + photoreactivation (*PR*) in transcriptionally active and inactive rDNA of W303.1a (*RAD1*).** Conditions were as described in Fig. 4. *TS*, transcribed strand; *NTS*, nontranscribed strand.

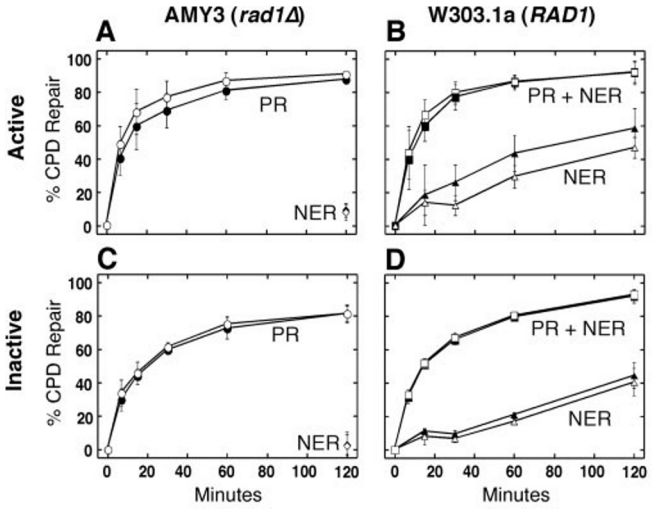


FIG. 6. **CPD repair in transcriptionally active and inactive rDNA.** Repair results are shown for the transcriptionally active fraction (*A* and *B*) and the inactive fraction (*C* and *D*) of AMY3 and W303.1a. *PR*, photoreactivation; *open symbols*, nontranscribed strand; *filled symbols*, transcribed strand. The curves are averages of three independent UV experiments and at least two gels per UV experiment.

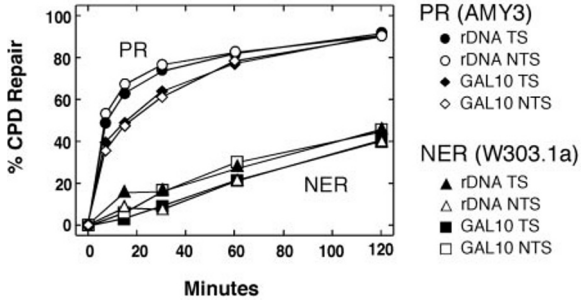


FIG. 7. **CPD repair in the *GAL10* gene and in total rDNA.** Cells were grown in glucose in which *GAL10* is repressed. Total rDNA was analyzed as described in Fig. 1. Repair of the coding region of *GAL10* (1.6-kb *Sal*I/*Eco*RI fragment) was analyzed as described previously (13). Data are averages of two gels of one repair experiment. *TS*, transcribed strand; *NTS*, nontranscribed strand; *PR*, photoreactivation.

Repair is intimately linked to chromatin structure and transcription. Nucleosomes restrict the accessibility of DNA and inhibit NER and photoreactivation, while transcription opens up chromatin, disrupts nucleosomes, and makes DNA more accessible (2, 43). It is therefore conceivable that DNA lesions that block RNA polymerases and thereby inactivate transcription might cause alterations in chromatin structure and consequently inhibit DNA repair. Alternatively the DNA repair process itself might be coupled to chromatin remodeling activities that alter chromatin as a consequence of repair (2, 4, 44). Thus, it is important to know how ribosomal genes are organized, how transcription affects the chromatin structure, and what consequences DNA lesions might have on the structural organization.

Active rRNA genes are depleted of nucleosomes, while inactive genes are folded in nucleosomes (27, 28, 36). Photolyase is an enzyme that strongly discriminates between nucleosomes and nucleosome-free DNA both *in vitro* and in yeast and therefore can be used as a tool to test whether DNA is folded in nucleosomes *in vivo* (9). Here we found that the inactive rDNA was repaired by photolyase as fast as the *GAL10* gene, which is packaged in nucleosomes when cells were grown in glucose (38). Thus the photoreactivation data are consistent with a nucleosomal conformation of inactive rRNA genes. Moreover, photoreactivation of the nontranscribed strand of the active rDNA was much faster than nucleosomal DNA (68% CPDs removed in 15 min compared with 45 and 50% in the inactive rDNA and *GAL10*, respectively). This is direct evidence obtained in live cells that rDNA of inactive genes is in a less accessible, nucleosomal conformation, while the active rRNA genes are in a more accessible, more open, and presumably non-nucleosomal conformation. In addition, the same photoreactivation data demonstrate that the *Nhe*I-released rDNA fragments maintained an open state after damage induction and during the time course of repair.

Cells can modulate the proportion of active and inactive rRNA gene copies in response to variations in environmental conditions (27, 45) implying that damage induction somewhere in the genome or in the rDNA could affect rRNA synthesis by varying the number of active gene copies. Psoralen cross-linking in mouse cells showed that the fraction of open (active) rDNA remained constant during repair, and there was no indication for chromatin rearrangements following UV damage formation (30). This is consistent with our observation that photolyase repairs active genes faster than inactive genes (see above). On the other hand, we made two observations that indicate that UV damage formation caused subtle alterations in chromatin accessibility. UV irradiation resulted in a reduction of *Nhe*I-released chromatin fragments, and psoralen cross-linking revealed a broad band in the released fraction consistent with a heterogeneous chromatin population. Thus, a fraction of the active rDNA was remodeled and suffered a structural change toward a more compact structure, which affected *Nhe*I and psoralen accessibility. However, UV irradi-

ation was not sufficient to convert all the active rDNA in an inaccessible (nucleosomal) state, although there was more than one lesion generated per transcribed region.

We do not know the structural basis for this transition. The non-nucleosomal state of transcribed rDNA is probably set up by the high density of transcribing RNA polymerases. If polymerases are blocked and transcription is stalled, it is possible that nucleosomes may form at random on the damaged genes. Heterogeneous psoralen cross-linking is expected if there are not enough histones available to package the whole gene. Alternatively it is possible that nucleosomes form only downstream of the blocked polymerase, while the upstream region is still challenged by re-initiation and transcription. Moreover, it is also conceivable that the reduced release of *Nhe*I fragments after UV damage formation could be caused by an array of polymerases formed because of a blocked polymerase further downstream. The blocked polymerase array, however, does not explain the heterogenous psoralen cross-linking population since RNAP-I was shown to be transparent to psoralen (46). It is also unlikely that the structural transitions are due to chromatin transitions in a narrow range around the *Nhe*I sites since the fraction of molecules containing a DNA lesion close to the *Nhe*I site is very small.

An additional observation related to chromatin structure was that the fraction of released genes recovered with increasing NER times but not with photoreactivation in the absence of NER. Since yeast photolyase in contrast to NER cannot repair 6-4PPs, it is possible that removal of 6-4PPs is a limiting process. 6-4PPs are generated at much lower yields than CPDs, but they are removed at a faster rate (18). One interpretation is that a fraction of rRNA genes resumes transcription elongation after the damage is removed and regenerates the normal open chromatin structure. This recovery scenario is independent of whether the damaged structure was due to (partial) coverage by nucleosomes or due to an array of stalled polymerases or both. If the recovery reflects only repair of the previously active rRNA genes, the recovery should be proportional to the repair kinetics. This is not supported by the data since no increase of released genes was observed in AMY3 (*rad1*Δ), although the major photoproducts, the CPDs, were almost completely repaired. We therefore should consider that the enhanced release of rDNA during NER could be an indirect effect of removal of DNA lesions from other parts of the genome. Only cells that are proficient in repair of 6-4PPs in transcription-blocked genes might be able to resume transcription and a normal metabolism including the activation of rRNA genes.

Previous studies have reported a strand bias of NER in bulk rDNA of yeast (33). We confirm this result and further demonstrate that the strand bias is due to preferential repair of the transcribed strand in the active fraction. This is evidence that transcription-coupled repair exists in genes transcribed by RNAP-I. Rad26 is involved in transcription-coupled repair of RNAP-II genes (47), but the strand bias in RNAP-I repair is independent of Rad26 (33). Thus, the molecular mechanisms for transcription-coupled repair of RNAP-I and RNAP-II genes are different. *In vitro* experiments established that human RNAP-I and RNAP-II are firmly blocked at CPDs on the transcribed strand but not by CPDs on the nontranscribed strand (48–51). The arrested RNAP-II inhibits access to photolyase (49) but neither inhibits nor stimulates repair by the human excision nuclease (50). To facilitate damage recognition and repair, the polymerases have to back off or dissociate from the lesion. Addition of elongation factor SII to arrested complexes releases RNAP-II from the lesion without disruption of the complex, shortens the transcript, and allows re-elongation after removal of the damage (49, 51). The human transcription release factor HuF2 very efficiently dissociates both RNAP-I and RNAP-II stalled at lesions (48). Thus, in doing so, the transcription elongation factors may influence the stability of the RNA polymerase complexes on the lesion and thereby influence damage verification and the repair process. Here we find that photolyase *in vivo* is only slightly inhibited in the transcribed strand of active rRNA genes, which is in contrast to the strong inhibition observed in the *GAL10* and *URA3* genes transcribed by RNAP-II (9, 13). Apparently photolyase has almost normal access to CPDs in transcribed strands of active rDNA. Different transcription rates are unlikely to explain that result since both the *GAL10* and rDNA genes are heavily transcribed (38, 52). Therefore, the photoreactivation data imply differential stability of RNAP-I and -II blocked at CPDs. The short persistence of RNAP-I at a lesion might reduce the recruitment of repair factors and provide an explanation for the weak strand bias of NER in active RNAP-I genes.

*Acknowledgments*—We thank Drs. J. Sogo, M. Muller, and R. Wellinger for experimental help and discussions and Dr. U. Suter for continuous support.

REFERENCES

1. Hoeijmakers, J. H. (2001) *Nature* **411,** 366–374
2. Thoma, F. (1999) *EMBO J.* **18,** 6585–6598
3. Smerdon, M. J., and Conconi, A. (1999) *Prog. Nucleic Acids Res. Mol. Biol.* **62,** 227–255
4. Moggs, J. G., and Almouzni, G. (1999) *Biochimie* (*Paris*) **81,** 45–52
5. Friedberg, E. C., Walker, G. C., and Siede, W. (1995) *DNA Repair and Mutagenesis*, ASM Press, Washington, D. C.
6. Sancar, A. (1996) *Science* **272,** 48–49
7. Yasui, A., Eker, A. P., Yasuhira, S., Yajima, H., Kobayashi, T., Takao, M., and Oikawa, A. (1994) *EMBO J.* **13,** 6143–6151
8. Sancar, G. B. (2000) *Mutat. Res.* **451,** 25–37
9. Suter, B., Livingstone, Z. M., and Thoma, F. (1997) *EMBO J.* **16,** 2150–2160
10. Suter, B., Schnappauf, G., and Thoma, F. (2000) *Nucleic Acids Res.* **28,** 4083–4089
11. Suter, B., Wellinger, R. E., and Thoma, F. (2000) *Nucleic Acids Res.* **28,** 2060–2068
12. Aboussekhra, A., and Thoma, F. (1998) *Genes Dev.* **12,** 411–421
13. Livingstone-Zatchej, M., Meier, A., Suter, B., and Thoma, F. (1997) *Nucleic Acids Res.* **25,** 3795–3800
14. Petit, C., and Sancar, A. (1999) *Biochimie* (*Paris*) **81,** 15–25
15. Prakash, S., and Prakash, L. (2000) *Mutat. Res.* **451,** 13–24
16. Tornaletti, S., and Hanawalt, P. C. (1999) *Biochimie* (*Paris*) **81,** 139–146
17. Wellinger, R. E., and Thoma, F. (1997) *EMBO J.* **16,** 5046–5056
18. Tijsterman, M., de Pril, R., Tasseron-de Jong, J. G., and Brouwer, J. (1999) *Mol. Cell. Biol.* **19,** 934–940
19. Tu, Y., Tornaletti, S., and Pfeifer, G. P. (1996) *EMBO J.* **15,** 675–683
20. Aboussekhra, A., and Thoma, F. (1999) *EMBO J.* **18,** 433–443
21. Mellon, I., Spivak, G., and Hanawalt, P. C. (1987) *Cell* **51,** 241–249
22. Smerdon, M. J., and Thoma, F. (1990) *Cell* **61,** 675–684
23. Sweder, K. S., and Hanawalt, P. C. (1992) *Proc. Natl. Acad. Sci. U. S. A.* **89,** 10696–10700
24. Dammann, R., and Pfeifer, G. P. (1997) *Mol. Cell. Biol.* **17,** 219–229
25. Carmo-Fonseca, M., Mendes-Soares, L., and Campos, I. (2000) *Nat. Cell Biol.* **2,** E107–E112
26. Conconi, A., Widmer, R. M., Koller, T., and Sogo, J. M. (1989) *Cell* **57,** 753–761
27. Dammann, R., Lucchini, R., Koller, T., and Sogo, J. M. (1993) *Nucleic Acids Res.* **21,** 2331–2338
28. Lucchini, R., and Sogo, J. M. (1998) in *Transcription of Ribosomal RNA Genes by Eukaryotic RNA Polymerase I* (Paule, M. R., ed) pp. 255–276, Springer-Verlag, Berlin
29. Christians, F. C., and Hanawalt, P. C. (1993) *Biochemistry* **32,** 10512–10518
30. Fritz, L. K., and Smerdon, M. J. (1995) *Biochemistry* **34,** 13117–13124
31. Christians, F. C., and Hanawalt, P. C. (1994) *Mutat. Res.* **323,** 179–187
32. Balajee, A. S., May, A., and Bohr, V. A. (1999) *Nucleic Acids Res.* **27,** 2511–2520
33. Verhage, R. A., Van de Putte, P., and Brouwer, J. (1996) *Nucleic Acids Res.* **24,** 1020–1025
34. Suter, B., Livingstone-Zatchej, M., and Thoma, F. (1999) *Methods Enzymol.* **304,** 447–461
35. Sherman, F., Fink, G. R., and Hicks, J. B. (1986) *Laboratory Course Manual for Methods in Yeast Genetics*, Cold Spring Harbor Laboratory, Cold Spring Harbor, NY
36. Muller, M., Lucchini, R., and Sogo, J. M. (2000) *Mol. Cell.* **5,** 767–777
37. Dammann, R., Lucchini, R., Koller, T., and Sogo, J. M. (1995) *Mol. Cell. Biol.* **15,** 5294–5303
38. Cavalli, G., and Thoma, F. (1993) *EMBO J.* **12,** 4603–4613
39. Leger-Silvestre, I., Trumtel, S., Noaillac-Depeyre, J., and Gas, N. (1999) *Chromosoma* **108,** 103–113
40. Fritz, L. K., Suquet, C., and Smerdon, M. J. (1996) *J. Biol. Chem.* **271,** 12972–12976
41. Stevnsner, T., May, A., Petersen, L. N., Larminat, F., Pirsel, M., and Bohr, V. A. (1993) *Carcinogenesis* **14,** 1591–1596

42. Vos, J. M., and Wauthier, E. L. (1991) *Mol. Cell. Biol.* **11,** 2245–2252
43. Orphanides, G., and Reinberg, D. (2000) *Nature* **407,** 471–475
44. Meijer, M., and Smerdon, M. J. (1999) *Bioessays* **21,** 596–603
45. Grummt, I. (1999) *Prog. Nucleic Acids Res. Mol. Biol.* **62,** 109–154
46. Sogo, J. M., Ness, P. J., Widmer, R. M., Parish, R. W., and Koller, T. (1984) *J. Mol. Biol.* **178,** 897–919
47. van Gool, A. J., Verhage, R., Swagemakers, S. M. A., Vandeputte, P., Brouwer, J., Troelstra, C., Bootsma, D., and Hoeijmakers, J. H. J. (1994) *EMBO J.* **13,** 5361–5369
48. Hara, R., Selby, C. P., Liu, M., Price, D. H., and Sancar, A. (1999) *J. Biol. Chem.* **274,** 24779–24786
49. Donahue, B. A., Yin, S., Taylor, J. S., Reines, D., and Hanawalt, P. C. (1994) *Proc. Natl. Acad. Sci. U. S. A.* **91,** 8502–8506
50. Selby, C. P., Drapkin, R., Reinberg, D., and Sancar, A. (1997) *Nucleic Acids Res.* **25,** 787–793
51. Tornaletti, S., Reines, D., and Hanawalt, P. C. (1999) *J. Biol. Chem.* **274,** 24124–24130
52. Cavalli, G., Bachmann, D., and Thoma, F. (1996) *EMBO J.* **15,** 590–597